

RESEARCH

Open Access



Promising approaches for the assembly of the catalytically active, recombinant *Desulfomicrobium baculatum* hydrogenase with substitutions at the active site

Malgorzata Witkowska¹, Robert P. Jedrzejczak², Andrzej Joachimiak², Onur Cavdar³, Anna Malankowska³, Piotr M. Skowron¹ and Agnieszka Zylicz-Stachula^{1*}

Abstract

Background Hydrogenases (H₂ases) are metalloenzymes capable of the reversible conversion of protons and electrons to molecular hydrogen. Exploiting the unique enzymatic activity of H₂ases can lead to advancements in the process of biohydrogen evolution and green energy production.

Results Here we created of a functional, optimized operon for rapid and robust production of recombinant [NiFe] *Desulfomicrobium baculatum* hydrogenase (Dmb H₂ase). The conversion of the [NiFeSe] Dmb H₂ase to [NiFe] type was performed on genetic level by site-directed mutagenesis. The native *dmb* operon includes two structural H₂ase genes, coding for large and small subunits, and an additional gene, encoding a specific maturase (protease) that is essential for the proper maturation of the enzyme. Dmb, like all H₂ases, needs intricate bio-production machinery to incorporate its crucial inorganic ligands and cofactors. Strictly anaerobic, sulfate reducer *D. baculatum* bacteria are distinct, in terms of their biology, from *E. coli*. Thus, we introduced a series of alterations within the native *dmb* genes. As a result, more than 100 elements, further compiled into 32 operon variants, were constructed. The initial requirement for a specific maturase was omitted by the artificial truncation of the large Dmb subunit. The assembly of the produced H₂ase subunit variants was investigated both, in vitro and in vivo. This approach resulted in 4 recombinant [NiFe] Dmb enzyme variants, capable of H₂ evolution. The aim of this study was to overcome the gene expression, protein biosynthesis, maturation and ligand loading bottlenecks for the easy, fast, and cost-effective delivery of recombinant [NiFe] H₂ase, using a commonly available *E. coli* strains.

Conclusion The optimized genetic constructs together with the developed growth and purification procedures appear to be a promising platform for further studies toward fully-active and O₂ tolerant, recombinant [NiFeSe] Dmb H₂ase, resembling the native Dmb enzyme. It could likely be achieved by selective cysteine to selenocysteine substitution within the active site of the [NiFe] Dmb variant.

Keywords Recombinant hydrogenase, Maturase, Metalloenzyme, Biohydrogen, Mutagenesis

*Correspondence:

Agnieszka Zylicz-Stachula
a.zylicz-stachula@ug.edu.pl

¹Department of Molecular Biotechnology, Faculty of Chemistry, University of Gdansk, Wita Stwosza 63, Gdansk 80-308, Poland

²Structural Biology Center, X-ray Science Division, Argonne National Laboratory, Argonne, IL 60439, USA

³Department of Environmental Technology, Faculty of Chemistry, University of Gdansk, Wita Stwosza 63, Gdansk 80-308, Poland



© The Author(s) 2023. **Open Access** This article is licensed under a Creative Commons Attribution 4.0 International License, which permits use, sharing, adaptation, distribution and reproduction in any medium or format, as long as you give appropriate credit to the original author(s) and the source, provide a link to the Creative Commons licence, and indicate if changes were made. The images or other third party material in this article are included in the article's Creative Commons licence, unless indicated otherwise in a credit line to the material. If material is not included in the article's Creative Commons licence and your intended use is not permitted by statutory regulation or exceeds the permitted use, you will need to obtain permission directly from the copyright holder. To view a copy of this licence, visit <http://creativecommons.org/licenses/by/4.0/>. The Creative Commons Public Domain Dedication waiver (<http://creativecommons.org/publicdomain/zero/1.0/>) applies to the data made available in this article, unless otherwise stated in a credit line to the data.

Introduction

Hydrogen (H₂) is considered an excellent, environmentally friendly energy carrier. The combustion of H₂ produces only heat and water vapour, contrary to traditional fossil fuels. Thus, it is gaining more and more attention as an alternative to oil and gas energy [1–3]. The industrial production of hydrogen is aided mostly with the intensive use of chemicals, toxic metals, and a vast amount of energy to maintain specified conditions. At the same time, H₂, as the most abundant element in the Universe, is widely exploited by living organisms in their energy conservation pathways [4].

Hydrogenases (H₂ases) are essential enzymes for the catalytic turnover of hydrogen, which are widely spread in a variety of organisms. These complex metalloenzymes catalyse the uptake and evolution of H₂. They are divided into several subclasses according to the metal content of the catalytic centre, as well as their phylogenetic and genetic features: (i) [Fe] hydrogenases, (ii) [FeFe] hydrogenases, and (iii) [NiFe] hydrogenases [5].

From the perspective of industrial applications, [NiFe] H₂ases could be particularly useful because they exhibit a high activity towards hydrogen evolution and are somewhat resistant to oxygen inactivation. [NiFe] H₂ases consist of at least two subunits. The large subunit (LH) of the [NiFe] H₂ases contains an active site with nickel and iron atoms, and a small subunit (SH) provides an electron transfer pathway with several, cubane [4Fe4S] or non cubane (like [4Fe3S] or [3Fe4S]) iron-sulphur clusters [6]. In the catalytic centre, nickel and iron coordinate CO and CN⁻ ligands that are rarely found in living organisms [6, 7]. Thus far, only a limited number of the successful, homologous or heterologous production of recombinant [NiFe] H₂ases have been reported [6, 8–10], due to their complex structures and maturation processes.

Among [NiFe] H₂ases, the specific [NiFeSe] subgroup is of a great interest. H₂ases belonging to this subgroup contain selenocysteine (symbol SeCys or U) instead of one of the cysteines (symbol Cys or C) at the active site. [NiFeSe] H₂ases, such as *D. baculatum* periplasmic hydrogenase (Dmb H₂ase), exhibit an enhanced oxygen tolerance and high H₂ evolution activity [11, 12]. It has been proposed that the role of selenium might be crucial due to its redox properties of Dmb H₂ase, when compared with sulphur [13]. The role of selenium in the catalytic center was examined by Marques et al. by creating a selenocysteine to cysteine variant of *Desulfovibrio vulgaris* Hildenborough (DvH) H₂ase. The recombinant enzyme was biosynthesized in a native organism and demonstrated lowered rates of nickel incorporation, which indicates that the selenium moiety plays a role in the maturation process. Nevertheless, this recombinant enzyme was still able to manifest some activity and inactive states characteristic of the [NiFe] type H₂ase [14].

Recently, Evans et al. confirmed the importance of a special position of selenocysteine of the [NiFe] Hyd-1 *E. coli* H₂ase for catalysis and O₂ tolerance. The studies were performed using a recent method for UAG-programmed site-specific Sec incorporation [15].

In *E. coli*, site-specific incorporation of SeCys into the biosynthesized polypeptide demands a dedicated set of enzymes, as well as the SeCys insertion sequence (SECIS element) – a strictly defined structure of translated mRNA template [16]. Unfortunately, incorporation of SECIS, while preserving the original DNA sequence, is not always possible. Even if the SECIS component is successfully introduced, obtaining the recombinant protein with positions fully occupied by SeCys is still highly challenging. Additionally, the mechanism behind the incorporation of iron and nickel atoms into the buried active site is complex and not entirely understood, with several proteins known to be essential for this process [17, 18]. However, this should not be a drawback for the heterologous expression of the [NiFeSe] H₂ase genes in *E. coli*, since *E. coli* itself produces several H₂ases and harbors a sufficient set of helper and accessory proteins. The maturation process of LH is finished with the cleavage of the C-terminal extension by a maturation protease, which is specific to a particular H₂ase [19]. Only after the LH cleavage occurs, SH can be assembled into functional complex [20]. Maturation of SH involves the synthesis and incorporation of cubane [4Fe4S] clusters. Two major systems – Isc and Suf – are responsible for Fe-S cluster biogenesis [21–23]. Their role is supposed to be partially interchangeable. It was shown, however, that widely used *E. coli* strains carry an in-frame gene fusion in the *suf* operon, impairing the efficiency of the cluster synthesis [24].

Although native Dmb H₂ase is secreted to periplasm, a specific DNA fragment, coding for a membrane translocation signal is present only in the SH coding gene. Interestingly, such a signal sequence directs the protein transport through the twin-arginine translocation (TAT) system, which allows for the secretion of fully folded proteins [25]. We hypothesize that the leader sequence of SH may serve for transportation of both assembled Dmb H₂ase subunits.

Thus far, Dmb H₂ase was only isolated from *D. baculatum* [26, 27]. Here, we investigated several possible strategies to solve the problems in heterologous H₂ase production, arising from the existing differences between a native host – *D. baculatum* and *E. coli*. Our approach resulted in dozens of the tested gene layouts. In this report, we describe a development of a promising strategy for the cloning, heterologous expression, and purification of the catalytically active Dmb H₂ase in a fast and simple manner.

Materials and methods

Plasmids and bacterial strains

All expression vectors used in this study were developed at the Midwest Center for Structural Genomics (MCSG). The description of the vectors is provided in Supplementary Material File 1. The combination of vectors gives flexible options for tag location and levels of protein expression while allowing for co-expression from two compatible origins of replication without time consuming artificial operon construction. The pMCSG53 expression vector generates a hexa-histidine tag upstream of a TEV recognition site at the N-termini of recombinant protein; this vector also harbors two genes coding for rare tRNAs - AGG/AGA for arginine and AUA for isoleucine [28, 29]. pRSF1 is used for the biosynthesis of protein variants without tags; its origin of replication - RSF1030 - enables the implementation of a two-plasmid system with ColE1 origin vectors. Plasmid pMCSG92 has similar properties to pMCSG53, but the protein of interest (POI) is biosynthesized with a TEV cleavage site and His₆-tag on the C-termini. pMCSG93 shares most of the pRSF1 functional features, but the TEV cleavage site preceding the His₆-tag is introduced at the C-terminus of the POI. Many of these vectors share the POIs adjacent sequence, which allows the same set of primers to be used for the cloning of the same insert into all the expression vectors. For a high throughput approach, ligation-independent cloning (LIC) was employed [30]. *E. coli* BL21-Gold(DE3) {F^{-ompT hsdS(r_B⁻ m_B⁻) dcm⁺ Tet^rgal λ(DE3) endA Hte} (Agilent Technologies) was used for the cloning procedures and for gene expression experiments. Cells were grown in liquid or on solid LB medium with 150 µg/ml ampicillin and 100 µg/ml kanamycin, when appropriate.}

Bioinformatics analysis, primer design, cloning methods

For the minimal *dmb* operon, three native genes from *D. baculatum* (Gene Bank Accession no. CP001629.1) were selected coding for: (i) large subunit (LH), (ii) small subunit (SH), and (iii) H2ase maturation protease (Hmp). The latter is vital for the final steps of enzyme maturation. For the prediction of transmembrane domains and signal sequences, online tools were used: Phobius [31] and PRED-TAT [32]. Gene sequences were codon optimized for *E. coli* as an expression host (see Supplementary Material File 2 for alignment of the native and optimized gene sequences). For the preparation of the designed recombinant constructs, the PCR cloning method and KOD Hot Start Polymerase (Novagen) were used. For the designing of the primers, a publicly available software tool, provided by the MCSG, was used [33]. PCR was conducted following the touch-down method (TD-PCR) guidelines [34]. DNA amplification schedule is provided in Supplementary Material File 1. PCR products were analyzed by agarose gel electrophoresis.

The selected, specific PCR fragments were purified from excess deoxynucleoside triphosphates (dNTPs) using Qiagen spin columns. Subsequently, inserts were treated with T4 DNA polymerase (NEB) and the corresponding dNTP. The prepared DNA inserts were annealed to the T4 DNA polymerase treated vectors and directly transformed into chemically competent *E. coli* cells.

Screening for positive bacterial clones and POIs biosynthesis

A single bacterial colony was picked from each transformation well and used as an inoculum for 1 ml of LB media with the appropriate antibiotic. Bacterial cells were grown at 37 °C with intense aeration. The next day, 1 ml of fresh LB medium was inoculated with the overnight culture and grown until OD₆₀₀ reached 1. Culture plates were chilled on ice to 19 °C and recombinant gene expression was induced with 1 mM IPTG. Upon induction, the following supplements were added: 1 mM MgCl₂, 50 µM NiSO₄, 25 µM FeCl₃. Cells were further cultured overnight at 18 °C with intense aeration (aerobic conditions) or, where indicated, purged with argon gas for 20 min and grown without shaking (anaerobic conditions). After a preliminary analysis, plasmid DNAs isolated from the selected bacterial clones were subjected to DNA sequencing. Protein expression was analyzed using polyacrylamide gel electrophoresis in denaturing conditions (SDS-PAGE) using Criterion TGX gels (Bio-Rad).

Screening for POIs solubility

Plates with the induced, overnight cultures were spun down, and the pellets were resuspended in 200 µl of lysis buffer (50 mM HEPES pH 8.0, 500 mM NaCl, 5% glycerol). The resulting suspension was frozen and sonicated in an ice bath in a cup-horn sonicator. Total protein samples were collected, and the plates were spun down for 60 min. Supernatants were mixed with Ni Sepharose (Ge Healthcare) and transferred to a 96-well filter plates. The resin was washed three times with 250 µl of lysis buffer with 20 mM imidazole and finally 40 µl of elution buffer (lysis buffer with 500 mM imidazole) was added to each well. The collected samples were analyzed by SDS-PAGE using Criterion TGX gels (Bio-Rad). If a detectable band of the correct molecular weight was observed after Coomassie-staining, the corresponding POI was scored for expression and solubility.

Spectrophotometric assay for hydrogenase enzymatic activity

The colorimetric assay of purified hydrogenase was conducted as based on the rate of the diametrical change in colour and extinction coefficient (ϵ MV) of methyl viologen (MV, Sigma) upon oxidation and measured at 600 nm [35, 36]. When MV is in its reduced form (MV^{•+}), its

extinction coefficient is $\epsilon=8.25$ ($\lambda=600$ nm) and the solution color is dark blue, while the oxidized form (MV^{2+}), the extinction coefficient is $\epsilon=0.0$ ($\lambda=600$ nm) and the solution is colorless. This method allows the indirect evaluation of hydrogenase activity as proton reduction is coupled to electron donor oxidation. Samples of purified enzyme were subjected to buffer exchange with Amicon centrifuge filters (Merck Millipore). 12 ml samples were concentrated twice to 0.5 ml and diluted with 50 mM phosphate buffer pH 7.0. After the second concentration, samples were diluted to a final concentration of 3 mg of protein/ml. 2 mM MV solution in 50 mM sodium phosphate pH 7.0 (reduced with 40 mM sodium dithionite) was prepared, and purged under argon for 15 min. 300 ng of protein (100 μ l) was mixed with 100 μ l of the MV solution, in 96-well clear bottom, black sided polystyrene microplate. The microplate was placed within a pre-cut tedlar bag, heat sealed, purged under argon for 15 min, and transferred to an anaerobic chamber, in which the measurements were conducted simultaneously with a Gene5 Microplate Reader (BioTek). Samples were prepared in triplicate and measurements were undertaken with shaking during a 6 min kinetic run with a measurement interval of 1 min. Control samples were prepared without sodium dithionite and without protein. A change in the absorbance during the time course of the test was calculated ($\Delta A_{600nm}/\Delta t$). The H₂ase activity towards hydrogen evolution (U) was calculated as μ moles H₂/min/mg of enzyme. The calculation was as follows:

$$U = \frac{(\text{dilution factor}) \left(\frac{\Delta A_{600nm}}{\Delta t} \right)}{(\epsilon_{600nm} \times l) \text{ (mg of enzyme used)}}$$

Photocatalytic hydrogen evolution assay

7.5 ml phosphate buffer was transferred to the Teflon reactor equipped with a quartz glass and cooling jacket and stirred with magnetic stirrer. The mixture was deaerated to remove the oxygen using nitrogen gas flow for 30 min. Finally, the pre-prepared syringe containing 7.5 ml mixture containing methyl viologen (MV^{2+}), L-cysteine and hydrogenase in an anaerobic tent was injected slowly into the reactor under nitrogen flow and purged for another 30 min. The final 15 ml reaction mixture with $MV^{2+} = 1.8$ mM, L-cysteine=18 mM and hydrogenase in 50 mM phosphate pH 7 buffer was then irradiated using a 1000 W Xenon lamp (Oriol, 66,021), which emitted both UV and visible irradiation. UV light was removed by a cut-off filter GG420 ($\lambda > 420$ nm). The temperature of the reactor was kept at 10°C by a thermostat. The zero sample was taken before light irradiation to detect the oxygen level in the reactor, which was always trace amount. At the end of 8 h of irradiation, 200 ml of gas samples were collected from the headspace of the photoreactor using

an air-tight syringe (Hamilton) and injected to the gas chromatograph (Thermo Scientific TRACE 1300-GC), coupled with thermal conductivity detector (TCD). The amount of hydrogen was calculated μ L per liter of the reaction mixture.

Results

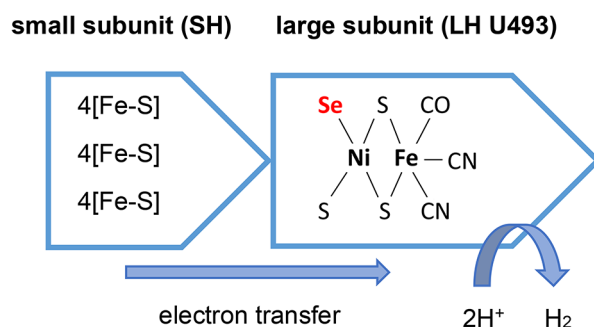
Construction of the components of the synthetic *dmb* operon

To obtain layouts containing all three genes of the minimal *dmb* operon, several variants of three synthetic genes encoding LH, SH, and maturation protease (*lh*, *sh*, *hmp* genes respectively) were designed and synthesized (Supplementary material File 3). Every gene of the minimal *dmb* operon was amplified with suitable primers in order to be inserted into the matching vector (pMCSG53, pRSF1, pMCSG92, pMCSG93) or as a subsequent synthetic operon. All primers used in this study are provided in Supplementary Material File 1.

Native Dmb enzyme belongs to the [NiFeSe] subgroup of H₂ases and contains SeCys in the active site. In *E. coli*, the insertion of the SeCys is driven by the appearance of the TGA (STOP) codon and requires the presence of the SECIS element. Unfortunately, the SECIS element for LH coding gene could not be recreated without altering the LH amino acid sequence. PCR reactions aiming to restore the SECIS element structure resulted in products highly 'toxic' for *E. coli* host and no expression of the recombinant genes was observed. To deal with this problem, we designed three different LH species: (a) U493M variant with SeCys replaced by methionine residue, (b) U493C variant with SeCys replaced by the Cys residue, as found in [NiFe] H₂ases (Fig. 1), and (c) U493STOP variant with a STOP codon inserted at position 493, resembling the native LH gene sequence, but without the presence of SECIS. Initially, the synthetic gene was designed as the U493M variant to obtain a full-length LH polipeptide (514 residues). Later, the gene was subjected to site-directed mutagenesis, and subsequently the U493C and U493STOP variants were obtained.

The performed expression experiments revealed that, in the case of all the investigated SH recombinant constructs, the solubility of the resulting SH protein variants was very low, regardless of the applied operon design and culture medium supplementation (Supplementary Material File 3). For that reason, two methods aimed at improving the solubility of the SH protein were applied: solubilization with urea and in vitro Fe-S cluster insertion [37]. The first of these methods was disruptive to the susceptible structure of cubane clusters, the second one was supposed to have low performance. However, the conducted experiments allowed for an improvement in the solubility of the selected SH variants (see Supplementary

a Native, periplasmic [NiFeSe] *Dmb* hydrogenase



b Recombinant, cytoplasmic [NiFe] *Dmb* hydrogenase

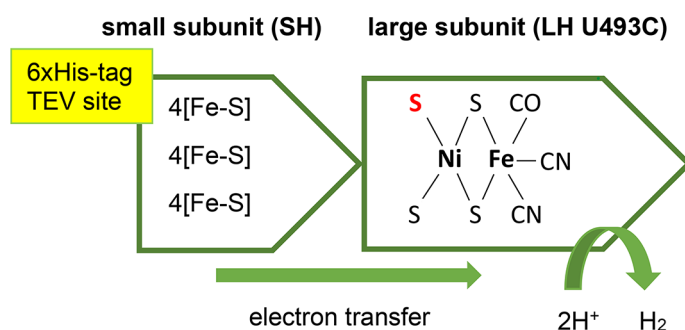


Fig. 1 Differences between the native and final, recombinant *Dmb* hydrogenase. **(a)** Schematic representation of the most prominent features of the native *Dmb* H₂ase. Selenium in the active centre is marked in red. **(b)** Schematic representation of the most prominent features of the recombinant *Dmb* H₂ase. The residues/amino acid position altered by mutagenesis (U493C) is marked in red. The N-terminal His₆-tag and TEV site, resulting from the expression from pMCSG53 vector, are shown in a yellow rectangle

Material File 4), which could be further used for the in vitro assembly of recombinant H₂ase.

Dmb H₂ase production via two-gene synthetic operon

Our original goal was to produce the active *Dmb* H₂ase using a three-gene synthetic operon. However, in the first step, we constructed and investigated properties of two-gene operons (Supplementary Material File 3, Sect. 1.2, Suppl. Table 2). For this purpose, two types of the ribosome binding site (RBS) were employed. Protein expression analysis of the several constructs showed low levels of the second gene expression. Moreover, it was observed that LH was not being cleaved, regardless of the chosen gene layout. Neither expression of the two-gene operon with both *lh* and *hmp* genes, nor co-expression of the genes using the separate recombinant constructs, resulted in the expected LH cleavage. Without the proper removal of the C-terminal section of the LH polypeptide, the subunit cannot form a heterodimer with SH. This step assures that SH subunit would

not be assembled with an inactive LH subunit structure and this is common throughout maturation schemes of phylogenetically distant H₂ases [38–40]. To address this problem, we decided to construct their truncated versions (Supplementary Material File 3). For each variant of LH (differing at position 493) we created its shorter counterpart (499 residues in length), with a C-terminal STOP codon (TAA). Employing the truncated LH-coding gene variants allowed us to remove the *hmp* gene from the operons (Supplementary Material File 3: Sect. 1.2). Such an approach eliminated the need to sustain overproduction of three proteins in the bacteria. The resulting constructs contained only two structural *dmb* genes (*lh* and *sh*). However, it was not clear whether the truncated LH species would be assembly competent with SH, as LH cleavage by Hmp is believed to be the final step in the [NiFe]-H₂ases maturation. To develop a fast and effective *Dmb* H₂ase purification procedure, we finally selected pMCSG53 as the expression vector (Supplementary Material File 1). Considering the above observed low

level of SH solubility, in vitro assembly of the truncated LH and the solubilized SH variant was performed, similarly to the method developed by Caserta et al. [41], who demonstrated that individually purified subunits of the *Ralstonia eutropha* [NiFe] H2ase could be assembled in vitro, forming a fully active enzyme. For in vitro assembly experiments, the separate recombinant bacterial cultures, producing LH variants with or without His₆-tag and SH variants with His₆-tag, were grown simultaneously. SH solubilization was performed and the resulting preparations were mixed in a 1:1 ratio prior to Immobilized Metal Affinity Chromatography (IMAC) purification.

Recombinant gene expression and purification of H2ase

For the enzymatic activity testing, the following gene layouts were chosen: (i) two-gene operons with the truncated *lh* gene variants (U493C, U493M, U493STOP), paired with the *sh dmb* gene and (ii) single subunit coding genes expressed in various compatible vectors. Cultures of *E. coli* harbouring the selected *dmb* genes were grown under intense aeration. From the tested variants, designs prepared in the pMCSG53 vector were selected as this vector provides a high yield of the POI with a cleavable

His₆-tag permitting fast protein purification. In case of the investigated two-gene operons (*sh* and *lh* genes in pMCSG53 vector), the biosynthesized SH subunit contained a cleavable N-terminal His₆-tag. Total protein samples were taken after overnight cultivations and analysed using SDS-PAGE. SH and LH U493M and U493C subunits, expressed from the single-gene layouts, are visible as dominant protein bands (Fig. 2A, lanes 1–6), similarly to U493STOP variant (Supplementary Material File 3, Sect. 1.1, Suppl. Tables 1 and Suppl. Figure 1). In the case of two-gene operons, the SH-corresponding band is more prominent than the band representing the subsequently translated LH subunit (Fig. 2A, lanes 7–8), which was observed for both U493C and U493M variants. Nevertheless, both subunits expressed together were in their soluble form (Fig. 2B, lanes 2 and 4). This eliminated an extensive and time consuming solubilization of SH.

Because H2ases are easily inactivated by oxygen species, as well as other factors, it is crucial to develop fast and simple purification procedures. A following protocol was developed: (i) sonication of the bacterial cells, (ii) vacuum aided IMAC purification, (iii) buffer exchange. IMAC purification was conducted in two stages, with a

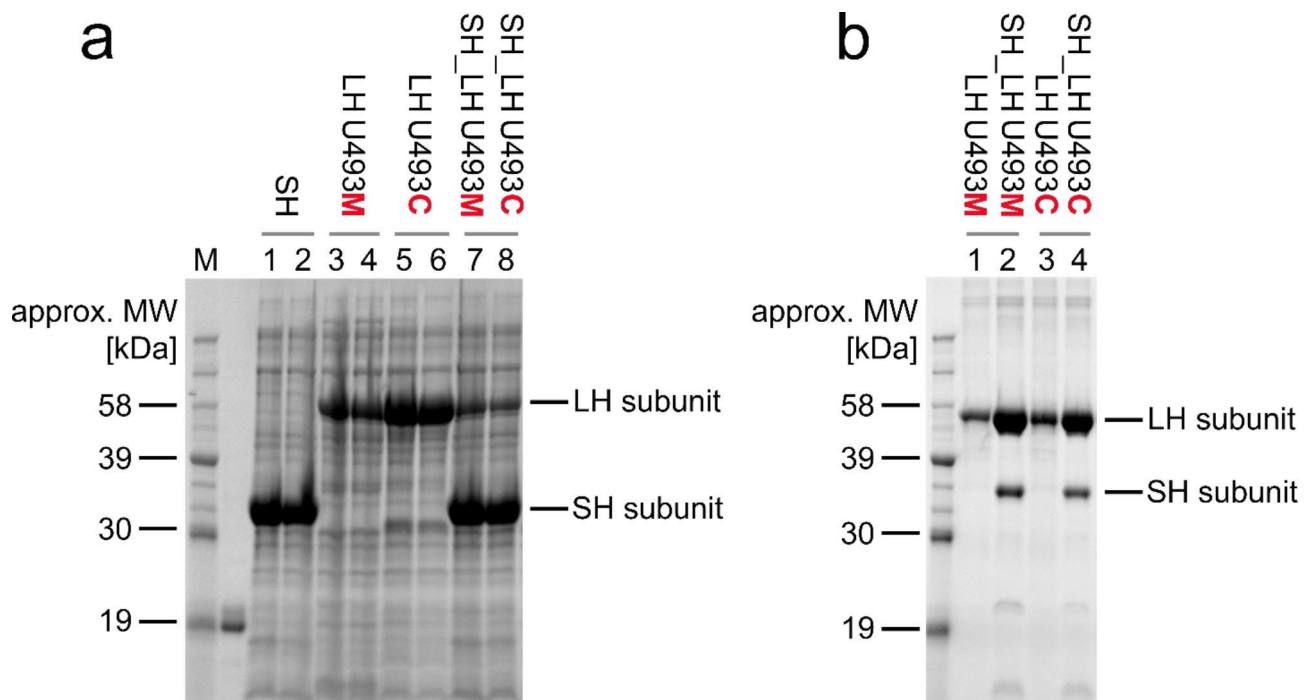


Fig. 2 Biosynthesis and isolation of the recombinant Dmb hydrogenase subunits from *E. coli*. After IPTG induction of the recombinant genes, the bacteria were further cultivated overnight at 18°C; approx. MW – approximate, theoretically predicted molecular weight. **(a)** Biosynthesis of the large (LH) and small (SH) recombinant Dmb H2ase subunits in *E. coli* BL21(DE3)Gold. Lane M, protein molecular weight ladder, selected bands marked; lanes 1–2, *E. coli* BL21(DE3)Gold [SH_pMCSG53]; lanes 3–4, *E. coli* BL21(DE3)Gold [LH U493M_pMCSG53]; lanes 5–6, *E. coli* BL21(DE3)Gold [LH U493C_pMCSG53]; lane 7, *E. coli* BL21(DE3)Gold [SH_LH U493M_pMCSG53]; lane 8, *E. coli* BL21(DE3)Gold [SH_LH U493C_pMCSG53]. **(b)** Isolation and Immobilized metal affinity chromatography (IMAC) purification of the recombinant Dmb H2ase subunits from *E. coli* BL21(DE3)Gold. All the purified protein variants were obtained using the recombinant pMCSG53 constructs. Lane M, protein molecular weight ladder, selected bands marked; lane 1, purified LH U493M; lane 2, purified SH and truncated LH U493M – expression from the operon; lane 3, purified truncated LH U493C; lane 4, purified SH and truncated LH U493C – expression from the operon

final 500 mM imidazole concentration in the elution buffer. Step (iii) is crucial for removing contaminants as well as imidazole from the sample buffer before a spectrophotometric activity assays.

H2ase activity measurements

Hydrogen evolution can be measured directly, for example by drawing a sample from the reaction mixture headspace ([42, 43], or indirectly by spectrophotometric measurement of change in absorbance. The indirect spectrophotometric methods recruit small-molecule dyes (oxidized or reduced by H2ases), such as benzyl viologen and methyl viologen [35, 36, 44–51]. For the spectrophotometric H2ase screening in multi-well plates, usually stoichiometric amounts of dithionite are used, or the H2 oxidation coupled to MV reduction in the absence of dithionite is tested. In this study, however, spectrophotometric measurements in the presence of excess dithionite were undertaken. The final preparations containing dimeric Dmb enzyme, obtained in vivo (via expression

Table 1 Comparison of the recombinant Dmb hydrogenase variant activities in the spectrophotometric methyl viologen assay

Construct (sample tested)	average hydrogenase activity [μ moles H ₂ /min/mg of protein]	standard deviation
LH U493C_STOP499_pMCSG53 + SH_pMCSG53 (in vitro assembly)	81.368	± 0.15
SH_rbs517_LH U493C_STOP499_pMCSG53 (in vivo assembly)	85.344	± 0.11
LH U493M_STOP499_pMCSG53 + SH_pMCSG53 (in vitro assembly)	28.644	± 0.11
SH_rbs517_LH U493M_STOP499_pMCSG53 (in vivo assembly)	38.278	± 0.01
LH U493M_STOP499_pMCSG53	0	0
LH U493C_STOP499_pMCSG53	0	0
SH_pMCSG53	0	0
assay buffer	0	0
<i>E. coli</i> BL21-Gold(DE3) strain (aerobic conditions)	0.0016	0
<i>E. coli</i> BL21-Gold(DE3) strain	0.0017	0

The recombinant Dmb H2ase preparations, containing 0.3 mg of the purified protein variant, were obtained via in vivo or in vitro assembly. The small H2ase subunit (SH) was subjected to a solubilization procedure prior to in vitro assembly. Single H2ase subunits: SH, LH U493C_STOP499 (truncated), LH U493M_STOP499 (truncated), prepared in a similar manner to the operon derived enzyme, showed no activity. A crude lysate from the *E. coli* BL21(DE3) Gold strain culture, which was grown in parallel with the IPTG induced recombinant Dmb H2ase producing cultures, was used as a negative control. An additional control sample of the strain, grown overnight in standard aerobic conditions, was also included. A sample of the assay buffer contained all of the components of the assay except the enzyme preparation/lysate. All the samples were prepared in triplicate and measurements were undertaken with shaking during 6 min kinetic runs with a measurement interval of 1 min.

of the two-gene operon) or by in vitro assembly of the separately purified subunits, were immediately purged with argon gas and assayed with an indirect hydrogen evolution assay using methyl viologen. A sample of *E. coli* BL21-Gold(DE3) lysate was used as a negative control. The enzymatic activity of single LH and SH subunits was also investigated as a form of negative control. The average activity towards H₂ evolution of the investigated samples is shown in Table 1. The results of the performed experiment indicate that the recombinant [NiFe] Dmb H2ase is capable of H₂ evolution. It should be noted, however, that in the presence of excess dithionite, MV cannot be easily oxidised by an active H2ase, potentially leading to false negative results.

The activity calculated for each measurement is shown in Table 1. The most active construct is the SH_LH U493C_pMCSG53 variant (expressed from a two-gene operon). Its' nucleotide and amino acid sequence, as well as map of the recombinant construct, are shown in Supplementary Material File 5. Surprisingly, constructs comprising of LH U493M and SH also exhibited significant activity, about half of that of the recombinant [NiFe] Dmb H2ase variant. In case of in vitro assembled subunits, expressed and biosynthesized separately and mixed prior to the assay, the calculated H₂ evolution activity is only slightly lower than for the operon derived Dmb enzyme (Table 1). The variant remains active even though SH purification was aided by urea solubilization, presumably affecting 4[Fe-S] cluster structures. No significant enzymatic activity was observed for the crude *E. coli* BL21(DE3)Gold lysates and single SH subunit. Interestingly, Caserta et al. recently demonstrated that the large subunit HoxC of the O₂-sensitive *Ralstonia eutropha* [NiFe] H2ase was capable of H₂ activation, although its activity was significantly lower compared to the native holoenzyme [52]. In contrast to the Caserta et al. results, no enzymatic activity of single LH Dmb subunit was detected using spectrophotometric methyl viologen assay.

To finally confirm the recombinant Dmb H2ase activity, photocatalytic evolution assay was performed. For that purpose, the most promising Dmb variant SH_LH U493C_pMCSG53 (selected using the spectrophotometric assay) was chosen (Table 1; Supplementary Material File 5). The performed experiment clearly indicated that the recombinant Dmb H2ase is capable of H₂ evolution (Fig. 3).

Discussion

A large number of H2ases, belonging to different classes, were cloned and isolated from native and closely related hosts [8]. However, heterologous expression of these enzymes often results in an inactive enzyme. Most active hydrogenases are isolated from organisms with specific

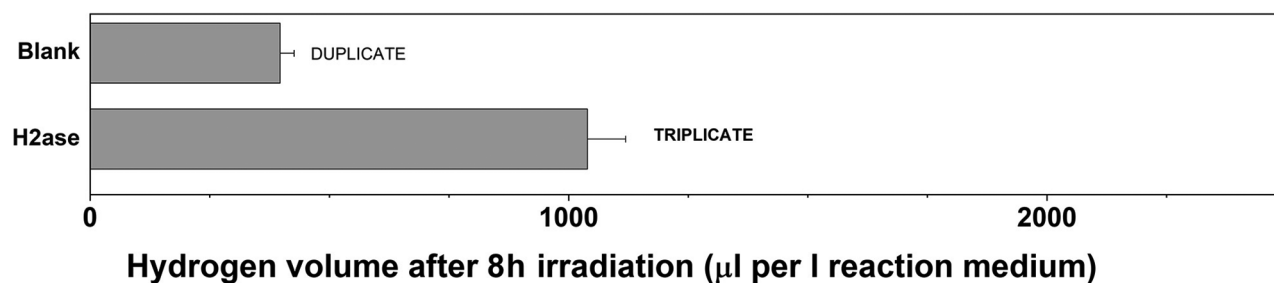


Fig. 3 Photocatalytic hydrogen evolution assay. The deaerated mixture containing methyl viologen, L-cysteine and SH_LH U493C_pMCSG53 hydrogenase variant was irradiated using a 1000 W Xenon lamp at 10°C. After 8 h of irradiation, 200 ml of gas samples were collected from the headspace of the photoreactor and injected to the gas chromatograph, coupled with thermal conductivity detector (TCD). The amount of hydrogen was calculated at µl per litre of the reaction mixture

demands for cultivation: anaerobes and extremophiles. Generally, we lack the molecular tools to easily manipulate those microbes, but also cultivation of these strains often demands very specialized equipment and complex strategies. Obtaining a high yield of POI from such cultures requires enormous effort. At the same time, the exact mechanism and features enhancing the abilities of H2ases are still poorly understood. In order to produce a considerable amount of enzyme for characterization, testing and application in photoinduced water splitting experiments, an efficient and easy to handle expression system is needed. To generate expression construct producing an active enzyme, dozens of layouts were tested.

In summary, *D. baculatum* periplasmic [NiFeSe] hydrogenase and hydrogenase maturation protease genes (3 genes) were optimized for heterologous expression in *E. coli*. 4 different expression vectors were employed and more than 100 constructs created (Supplementary Material File 3). Site directed mutagenesis was performed to obtain all the designed LH variants. The resulting constructs were arranged in two-gene or three-gene synthetic operons (37 different layouts) (Supplementary Material File 3, Sect. 1.2 and 1.3). The need for specific protease (maturase) during Dmb hydrogenase maturation was dismissed by introduction of artificial truncation of the LH gene sequence, by means of mutagenesis. Out of the tested variants and designs, two operons: SH_LH U493M_pMCSG53 and SH_LH U493C_pMCSG53 resulted in a soluble H2ase with activity towards H₂ evolution. These constructs differ from each other with the amino acid residue placed in position 493 of the polypeptide. In the native enzyme, this position is occupied by selenocysteine, encoded by the TGA codon. During translation, a specific structure (SECIS), following the TGA codon, determines an insertion of suitable amino acid instead of termination of the process. The *E. coli* SECIS structure differs from the one from *D. baculatum*, thus the incorporation of SeCys is not possible without interference in the H2ase structure. Attempts to create the SECIS element in the U493STOP mutant failed due

to the high toxicity of the construct and immediate cell lysis after induction of the recombinant operon expression. Therefore, we constructed the U493C LH variant, which resulted in production of a partially active [NiFe] instead of [NiFeSe] hydrogenase. Unexpectedly, the other variant U493M of Dmb H2ase, which will be used in future for the planned experiments with selenomethionine insertion (this can be achieved simply by addition of the selenomethionine to the culture media), also exhibited some H2ase activity. This phenomenon should be further investigated, as no simple explanation for the role of methionine in the catalytic centre can be readily provided. Our results (concerning the U493C LH variant) corroborate with the results presented by Marques et al. [14], who constructed, characterized, and crystalized the U489C variant of the DvH NiFeSe H2ase, converting [NiFeSe] H2ase to a partially active [NiFe] enzyme. Interestingly, the U489C variant appeared to be Ni-depleted, revealing crucial involvement of SecCys residue in the enzyme maturation. In addition, Marques et al. showed that the active site of the purified U489C variant could be partially reconstituted by incubation with NiCl₂ under H₂.

The biosynthesis of SH turned out to be another drawback in this study. Typically for solubilization of this protein in vitro, a 2 M urea wash was used, followed by Fe-S cluster incorporation. However, the problem with low SH solubility was solved by co-expression of the SH encoding gene from a single operon with the truncated version of LH gene (Supplementary Material File 3).

While several vectors were used in this study, providing the POIs with or without His₆-tag on either termini, the recombinant gene expression level, obtained for vector pMCSG53, seemed to exceed the others. Additionally, the resulting N-terminal His₆-tag extension was crucial to reduce the time of the isolation procedure. Immediately after the purification step, activity tests were performed. We have aimed for a minimal number of steps and maximum reduction of time between bacterial pellet collection and further experiments with the enzymes.

During purification, anaerobic conditions were not strictly maintained, thus the assayed H₂ases experienced short periods of O₂ exposure. A fast and simple protocol of purification of the recombinant [NiFe] Dmb H₂ase, applicable for the production of active enzyme, even after short O₂ exposure, was developed. It was previously shown that [NiFeSe] H₂ases are able to recover after oxygen inactivation. Although the U493C variant remained active despite short O₂ exposure during the purification process, it is probably less stable after O₂ inactivation than the native [NiFeSe] H₂ase. During the assay, only a small difference in calculated activity was visible between the enzyme variant assembled in vitro and in vivo. On the one hand, this proves the efficacy of the solubilization procedure, on the other hand it might be the result of Fe-S cluster inactivation by the applied conditions. In the future, the influence of purification procedure on the iron content in the recombinant Dmb H₂ase could be investigated with spectroscopic studies.

According to literature, the specific activity of the native [NiFeSe] Dmb H₂ase was found to be 500–2000 μmol H₂/min/mg, depending on the culture medium, enzyme preparation and the H₂ evolution assay [11, 26, 53, 54]. Although the performed assays indicated that the recombinant [NiFe] Dmb H₂ase is capable of H₂ evolution, experiments using direct electrochemical methods or gas chromatography should be performed to evaluate the enzyme properties. It needs to be stated that the enzyme exhibits only a fraction of the native [NiFeSe] Dmb H₂ase activity. Further studies need also to be carried out to improve the recombinant enzyme capabilities. Among them, the site-specific UAG-programmed Sec insertion is planned to reconstitute the active site of the [NiFeSe] enzyme, as it was done for the [NiFe] Hyd-1 H₂ase [55]. Additionally, biosynthesis of the recombinant Dmb H₂ase subunits in other *E. coli* strains, such as derivatives of K-12 (which do not have issues in terms of nickel transport) or co-production of the *D. baculatum* Hyp maturation proteins may be considered to increase the catalytic activity of the recombinant Dmb H₂ase. Such a strategy has been recently employed by Fan et al. to produce catalytically active, recombinant [NiFe] hydrogenase from *Cupriavidus necator* in *E. coli* [8]. Our future studies will also concern investigation of the iron content in the active site pocket of the isolated U493C LH subunit. Although, we did not observed catalytic activity of this subunit, it is possible that incubation of the purified protein with NiCl₂ under H₂ [14] may lead to reconstitution of its active site and potential conversion to minimal H₂ase, similar to the catalytically competent, large subunit HoxC of the O₂-sensitive [NiFe]-hydrogenase, derived from *Ralstonia eutropha* [52].

Conclusions

Catalytically active recombinant [NiFe] Dmb H₂ase may be biosynthesized in *E. coli* by co-expression of the SH encoding gene and the truncated version of the LH gene, organized into a single operon. Substitution of selenocysteine to cysteine in LH subunit results in production of an active [NiFe] instead of [NiFeSe] H₂ase. The proposed approach could be advantageous for other H₂ases, enabling the establishment of the minimal pathway for enzyme maturation.

Supplementary Information

The online version contains supplementary material available at <https://doi.org/10.1186/s12934-023-02127-w>.

Additional file 1: Primer sequences, thermal cycling schedule and protein expression vectors.

Additional file 2: Aligned sequences of native and optimized synthetic genes.

Additional file 3: Detailed experimental results concerning cloning, expression and purification of the Dmb operon components. 1.1. Separate cloning of the Dmb operon components. 1.2. Production of protein complexes via two genes layouts. 1.3. Production of hydrogenase complex via co-expression of three-piece operon elements. 1.4. Production of hydrogenase complex via in vitro assembly. 1.5. Periplasmic transport signal modifications and large subunit truncation. 1.6. Production of hydrogenase complex via co-expression of two-piece operon elements. 1.7. Optimization of the small subunit solubility. 1.8. Hydrogenase assembly in optimized conditions. 1.9. Production of hydrogenase complex via expression of two-piece operon elements.

Additional file 4: Procedures for the solubilization of SH constructs and for in vitro Fe-S clusters insertion.

Additional file 5: Genetic map and DNA sequence of the Dmb hydrogenase SH_LH_U493C_pMCSG53 recombinant construct.

Acknowledgements

Joanna Zebrowska is highly appreciated for critical reading of the Supplementary material file 3.

Authors' contributions

Conceptualization: PMS, AZS, JR; design and methodology: RJ and MW; most laboratory experiments: MW; photocatalytic hydrogen evolution: AM, OC; interpretation of the experimental data: MW, JR, AJ, PMS, AZS; supervision: RJ, AZS, AJ; funding acquisition AJ, AM, PMS; writing: MW and AZS. All authors contributed to the article and approved the submitted version.

Funding

This work was supported by Polish National Science Centre Grant for project titled: Photo-bio hydrogen production by [NiFe] hydrogenase-MNPs/SiO₂/MaSb hybrids under visible light irradiation (2016/23/D/ST8/02682), National Centre for Research and Development POWR.03.02.00-IP.08-00-DOK/16, Polish Ministry of Science and Higher Education DS 531-T040-D839-22, DS 531-T040-D839-23, DS 531-T020-D845-23 and in part by National Institutes of Health Grant GM115586 and by the U.S. Department of Energy, Office of Biological and Environmental Research, under contract DE-AC02-06CH11357 for the Midwest Center for Structural Genomics Community Resource.

Data availability

The datasets used and/or analysed during the current study are available from the corresponding author on reasonable request.

Declarations

Competing interests

The authors declare no competing interests.

Conflict of interest

The authors declare that the research was conducted in the absence of any commercial or financial relationships that could be construed as a potential conflict of interest.

Received: 22 March 2023 / Accepted: 17 June 2023

Published online: 21 July 2023

References

- Rüdiger O, de Lacey AL, Fernández VM, Cammack R. Hydrogenases and alternative energy strategies. In: Handbook of Green Chemistry. 2010. <https://doi.org/10.1002/9783527628698.hgc032>.
- Sanchez MLK, Wu CH, Adams MWW, Brian Dyer R. Optimizing electron transfer from CdSe QDs to hydrogenase for photocatalytic H₂ production. *Chem Commun.* 2019;55(39). <https://doi.org/10.1039/c9cc01150a>.
- Magnuson A, Mamedov F, Messinger J. Toward sustainable H₂ production: linking hydrogenase with photosynthesis. *Joule.* 2020;4(6). <https://doi.org/10.1016/j.joule.2020.05.014>.
- Schoelmerich MC, Müller V. Energy conservation by a hydrogenase-dependent chemiosmotic mechanism in an ancient metabolic pathway. *Proc Natl Acad Sci U S A.* 2019;116(13). <https://doi.org/10.1073/pnas.1818580116>.
- Greening C, Biswas A, Carere CR, Jackson CJ, Taylor MC, Stott MB, et al. Genomic and metagenomic surveys of hydrogenase distribution indicate H₂ is a widely utilised energy source for microbial growth and survival. *ISME J.* 2016;10(3). <https://doi.org/10.1038/ismej.2015.153>.
- Vignais PM, Billoud B. Occurrence, classification, and biological function of hydrogenases: An overview. *Chem Rev [Internet].* 2007 Oct 1;107(10):4206–72. <https://doi.org/10.1021/cr050196r>.
- Reissmann S, Hochleitner E, Wang H, Paschos A, Lottspeich F, Glass RS, et al. Taming of a poison: biosynthesis of the NiFe-hydrogenase cyanide ligands. *Sci (1979).* 2003;299(5609). <https://doi.org/10.1126/science.1080972>.
- Fan Q, Neubauer P, Lenz O, Gimpel M. Heterologous hydrogenase overproduction systems for biotechnology—an overview. *Int J Mol Sci.* 2020;21. <https://doi.org/10.3390/ijms21165890>.
- Fan Q, Waldburger S, Neubauer P, Riedel SL, Gimpel M. Implementation of a high cell density fed-batch for heterologous production of active [NiFe]-hydrogenase in *Escherichia coli* bioreactor cultivations. *Microb Cell Fact.* 2022 Dec 1;21(1). <https://doi.org/10.1186/s12934-022-01919-w> PMID: 36123684.
- Fan Q, Caserta G, Lorent C, Zebger I, Neubauer P, Lenz O et al. High-Yield Production of Catalytically Active Regulatory [NiFe]-Hydrogenase From *Cupriavidus necator* in *Escherichia coli*. *Front Microbiol.* 2022 Apr 29;13. <https://doi.org/10.3389/fmicb.2022.894375> PMID: 35572669.
- Parkin A, Goldet G, Cavazza C, Fontecilla-Camps JC, Armstrong FA. The difference a Se makes? Oxygen-tolerant hydrogen production by the [NiFeSe]-hydrogenase from *Desulfomicrobium baculatum*. *J Am Chem Soc.* 2008;130(40). <https://doi.org/10.1021/ja803657d>.
- Wombwell C, Caputo CA, Reisner E. [NiFeSe]-hydrogenase chemistry. *Acc Chem Res.* 2015;48(11). <https://doi.org/10.1021/acs.accounts.5b00326>.
- Volbeda A, Amara P, Iannello M, de Lacey AL, Cavazza C, Carlos Fontecilla-Camps J. Structural foundations for the O₂ resistance of *Desulfomicrobium baculatum* [NiFeSe]-hydrogenase. *Chem Commun.* 2013;49(63). <https://doi.org/10.1039/c3cc43619e>.
- Marques MC, Tapia C, Gutiérrez-Sanz O, Ramos AR, Keller KL, Wall JD et al. The direct role of selenocysteine in [NiFeSe] hydrogenase maturation and catalysis. *Nature Chemical Biology* 2017 13:5 [Internet]. 2017 Mar 20 [cited 2023 Apr 14];13(5):544–50. <https://doi.org/10.1038/nchembio.2335> PMID: 28319099.
- Mukai T, Sevostyanova A, Suzuki T, Fu X, Söll D. A Facile Method for Producing Selenocysteine-Containing Proteins. *Angewandte Chemie International Edition [Internet].* 2018 Jun 11 [cited 2023 Apr 19];57(24):7215–9. <https://doi.org/10.1002/anie.201713215> PMID: 29631320.
- Berry MJ, Banu L, Chen Y, Mandel SJ, Kieffer JD, Harney JW, et al. Recognition of UGA as a selenocysteine codon in type I diiodinase requires sequences in the 3' untranslated region. *Nature.* 1991;353(6341). <https://doi.org/10.1038/353273a0>.
- Lacasse MJ, Zamble DB. [NiFe]-Hydrogenase maturation. Vol. 55, *Biochemistry.* 2016. <https://doi.org/10.1021/acs.biochem.5b01328>.
- Miki K, Atomi H, Watanabe S. Structural insight into [NiFe] hydrogenase maturation by transient complexes between hyp proteins. *Acc Chem Res.* 2020;53(4). <https://doi.org/10.1021/acs.accounts.0c00022>.
- Senger M, Stripp ST, Soboh B. Proteolytic cleavage orchestrates cofactor insertion and protein assembly in [NiFe]-hydrogenase biosynthesis. *J Biol Chem.* 2017;292(28). <https://doi.org/10.1074/jbc.M117.788125>.
- Thomas C, Muhr E, Sawers RG. Coordination of synthesis and assembly of a modular membrane-associated [NiFe]-hydrogenase is determined by cleavage of the C-terminal peptide. *J Bacteriol.* 2015;197(18). <https://doi.org/10.1128/JB.00437-15>.
- Pérard J, Ollagnier de Choudens S. Iron–sulfur clusters biogenesis by the SUF machinery: close to the molecular mechanism understanding. *J Biol Inorg Chem.* 2018;23. <https://doi.org/10.1007/s00775-017-1527-3>.
- Pérard J, Ollagnier de Choudens S. Correction to: Iron–sulfur clusters biogenesis by the SUF machinery: close to the molecular mechanism understanding (JBIC Journal of Biological Inorganic Chemistry, (2018), 23, 4, (581–596), <https://doi.org/10.1007/s00775-017-1527-3>). Vol. 23, *Journal of Biological Inorganic Chemistry.* 2018. <https://doi.org/10.1007/s00775-018-1571-7>.
- Baussier C, Fakroun S, Aubert C, Dubrac S, Mandin P, Py B, et al. Making iron-sulfur cluster: structure, regulation and evolution of the bacterial ISC system. *Adv Microb Physiol.* 2020;76. <https://doi.org/10.1016/bs.ampbs.2020.01.001>.
- Corless EI, Mettert EL, Kiley PJ, Antony E. Elevated expression of a functional suf pathway in *Escherichia coli* BL21(DE3) enhances recombinant production of an iron-sulfur cluster-containing protein. *J Bacteriol.* 2020;202(3). <https://doi.org/10.1128/JB.00496-19>.
- Palmer T, Berks BC. The twin-arginine translocation (Tat) protein export pathway. *Nat Rev Microbiol.* 2012;10. <https://doi.org/10.1038/nrmicro2814>.
- Teixeira M, Fauque G, Moura I, Lespinat PA, Berlier Y, Prickril B, et al. Nickel-[iron-sulfur]-selenium-containing hydrogenases from *Desulfotomobium baculatus* (DSM 1743): Redox centers and catalytic properties. *Eur J Biochem.* 1987;167(1). <https://doi.org/10.1111/j.1432-1033.1987.tb13302.x>.
- Garcin E, Vernede X, Hatchikian EC, Volbeda A, Frey M, Fontecilla-Camps JC. The crystal structure of a reduced [NiFeSe] hydrogenase provides an image of the activated catalytic center. *Structure.* 1999;7(5). [https://doi.org/10.1016/S0969-2126\(99\)80072-0](https://doi.org/10.1016/S0969-2126(99)80072-0).
- Eschenfeldt WH, Lucy S, Millard CS, Joachimiak A, Mark ID. A family of LIC vectors for high-throughput cloning and purification of proteins. *Methods Mol Biol.* 2009;498. https://doi.org/10.1007/978-1-59745-196-3_7.
- Eschenfeldt WH, Makowska-Grzyska M, Stols L, Donnelly MI, Jedrzejczak R, Joachimiak A. New LIC vectors for production of proteins from genes containing rare codons. *J Struct Funct Genomics.* 2013;14(4). <https://doi.org/10.1007/s10969-013-9163-9>.
- Stevenson J, Krycer JR, Phan L, Brown AJ. A practical comparison of ligation-independent cloning techniques. *PLoS ONE.* 2013;8(12). <https://doi.org/10.1371/journal.pone.0083888>.
- Käll L, Krogh A, Sonnhammer ELL. Advantages of combined transmembrane topology and signal peptide prediction—the Phobius web server. *Nucleic Acids Res.* 2007;35(SUPPL2). <https://doi.org/10.1093/nar/gkm256>.
- Bagos PG, Nikolaou EP, Liakopoulos TD, Tsirigos KD. Combined prediction of Tat and Sec signal peptides with hidden Markov models. *Bioinformatics.* 2010;26(22). <https://doi.org/10.1093/bioinformatics/btq530>.
- Yoon JR, Laible PD, Gu M, Scott HN, Collart FR. Express primer tool for high-throughput gene cloning and expression. *Biotechniques.* 2002;33(6). <https://doi.org/10.2144/02336bc03>.
- Green MR, Sambrook J. Touchdown polymerase chain reaction (PCR). *Cold Spring Harb Protoc.* 2018;2018(5). <https://doi.org/10.1101/pdb.prot095133>.
- Yu L, Wolin MJ. Hydrogenase measurement with photochemically reduced methyl viologen. *J Bacteriol.* 1969;98(1). <https://doi.org/10.1128/jb.98.1.51-55.1969>.
- Ren YL, Xing XH, Zhang C, Gou ZX. A simplified method for assay of hydrogenase activities of H₂ evolution and uptake in *Enterobacter aerogenes*. *Biotechnol Lett.* 2005;27(14). <https://doi.org/10.1007/s10529-005-8106-3>.
- Külzer R, Pils T, Kappl R, Hüttermann J, Knappe J. Reconstitution and characterization of the polynuclear iron-sulfur cluster in pyruvate formate-lyase-activating enzyme: molecular properties of the holoenzyme form. *J Biol Chem.* 1998;273(9). <https://doi.org/10.1074/jbc.273.9.4897>.
- Peters JW, Schut GJ, Boyd ES, Mulder DW, Shepard EM, Broderick JB et al. [FeFe]- and [NiFe]-hydrogenase diversity, mechanism, and maturation.

- Biochimica et Biophysica Acta (BBA) - Molecular Cell Research. 2015 Jun 1;1853(6):1350–69. <https://doi.org/10.1016/j.bbamcr.2014.11.021> PMID: 25461840.
39. Nicolet Y, Rubach JK, Posewitz MC, Amara P, Mathevon C, Atta M et al. X-ray structure of the [FeFe]-hydrogenase maturase HydE from *Thermotoga maritima*. *Journal of Biological Chemistry* [Internet]. 2008 Jul 4 [cited 2023 Apr 19];283(27):18861–72. <https://doi.org/10.1074/jbc.M801161200> PMID: 18400755.
40. Kuchenreuther JM, Britt RD, Swartz JR. New Insights into [FeFe] Hydrogenase Activation and Maturase Function. *PLoS One* [Internet]. 2012 Sep 25 [cited 2023 Apr 19];7(9):e45850. <https://doi.org/10.1371/JOURNAL.PONE.0045850> PMID: 23049878.
41. Caserta G, Lorent C, Pelmenschikov V, Schoknecht J, Yoda Y, Hildebrandt P et al. In Vitro Assembly as a Tool to Investigate Catalytic Intermediates of [NiFe]-Hydrogenase. *ACS Catal* [Internet]. 2020 Dec 4 [cited 2023 Apr 19];10(23):13890–4. https://doi.org/10.1021/ACSCATAL.0C04079/SUPPL_FILE/C50C04079_SI_002.ZIP.
42. Krassen H, Stripp S, von Abendroth G, Ataka K, Happe T, Heberle J. Immobilization of the [FeFe]-hydrogenase CrHydA1 on a gold electrode: Design of a catalytic surface for the production of molecular hydrogen. *J Biotechnol*. 2009 Jun 1;142(1):3–9. <https://doi.org/10.1016/j.jbiotec.2009.01.018> PMID: 19480942.
43. Engelbrecht V, Liedtke K, Rutz A, Yadav S, Günzel A, Happe T. One isoform for one task? The second hydrogenase of *Chlamydomonas reinhardtii* prefers hydrogen uptake. *Int J Hydrogen Energy* 2021 Feb 8;46(10):7165–75. <https://doi.org/10.1016/j.ijhydene.2020.11.231>.
44. Ballantine SP, Boxer DH. Nickel-containing hydrogenase isoenzymes from anaerobically grown *Escherichia coli* K-12. *J Bacteriol* [Internet]. 1985 [cited 2023 May 24];163(2):454–9. <https://doi.org/10.1128/JB.163.2.454-459.1985> PMID: 3894325.
45. PECK HD, GEST H. A NEW PROCEDURE FOR ASSAY OF BACTERIAL HYDROGENASES. *J Bacteriol* [Internet]. 1956 Jan [cited 2023 May 24];71(1):70. <https://doi.org/10.1128/JB.71.1.70-80.1956> PMID: 13286232.
46. Lacasse MJ, Douglas CD, Zamble DB. Mechanism of Selective Nickel Transfer from HypB to HypA, *Escherichia coli* [NiFe]-Hydrogenase Accessory Proteins. *Biochemistry* [Internet]. 2016 Dec 13 [cited 2023 May 24];55(49):6821–31. <https://doi.org/10.1021/ACS.BIOCHEM.6B00706> PMID: 27951644.
47. Zhang JW, Butland G, Greenblatt JF, Emili A, Zamble DB. A role for SlyD in the *Escherichia coli* hydrogenase biosynthetic pathway. *J Biol Chem* [Internet]. 2005 Feb 11 [cited 2023 May 24];280(6):4360–6. <https://doi.org/10.1074/JBC.M411799200> PMID: 15569666.
48. Douglas CD, Ngu TT, Kaluarachchi H, Zamble DB. Metal transfer within the *Escherichia coli* HypB-HypA complex of hydrogenase accessory proteins. *Biochemistry* [Internet]. 2013 Sep 2 [cited 2023 May 24];52(35):6030–9. <https://doi.org/10.1021/BI400812RPMID:23899293>.
49. Palmer T, Berks BC, Sargent F. Analysis of Tat targeting function and twin-arginine signal peptide activity in *Escherichia coli*. *Methods Mol Biol* [Internet]. 2010 [cited 2023 May 24];619:191–216. https://doi.org/10.1007/978-1-60327-412-8_12 PMID: 20419412.
50. Lacasse MJ, Sebastiampillai S, Côté JP, Hodkinson N, Brown ED, Zamble DB. A whole-cell, high-throughput hydrogenase assay to identify factors that modulate [NiFe]-hydrogenase activity. *J Biol Chem* [Internet]. 2019 Oct 18 [cited 2023 May 24];294(42):15373–85. <https://doi.org/10.1074/JBC.RA119.008101> PMID: 31455635.
51. Chongdar N, Pawlak K, Rüdiger O, Reijerse EJ, Rodríguez-Maciá P, Lubitz W et al. Spectroscopic and biochemical insight into an electron-bifurcating [FeFe] hydrogenase. *J Biol Inorg Chem* [Internet]. 2020 Feb 1 [cited 2023 May 25];25(1):135–49. <https://doi.org/10.1007/S00775-019-01747-1> PMID: 31823008.
52. Caserta G, Lorent C, Ciaccavava A, Keck M, Breglia R, Greco C et al. The large subunit of the regulatory [NiFe]-hydrogenase from *Ralstonia eutropha* – a minimal hydrogenase? *Chem Sci* [Internet]. 2020 Jun 3 [cited 2023 Apr 14];11(21):5453–65. <https://doi.org/10.1039/D0SC01369B>.
53. Fauque G, Peck HD, Moura JGG, Huynh BH, Berlier Y, DerVartanian DV et al. The three classes of hydrogenases from sulfate-reducing bacteria of the genus *Desulfovibrio*. *FEMS Microbiol Lett*. 1988 Dec;54(4):299–344. [https://doi.org/10.1016/0378-1097\(88\)90248-0](https://doi.org/10.1016/0378-1097(88)90248-0) PMID: 3078655.
54. He SH, Teixeira M, LeGall J, Patil DS, Moura I, Moura JJ, et al. EPR studies with 77Se-enriched (NiFeSe) hydrogenase of *Desulfovibrio baculatus*. Evidence for a selenium ligand to the active site nickel. *J Biol Chem* [Internet]. 1989;264(5):2678–82. PMID: 2536719.
55. Evans RM, Krahn N, Murphy BJ, Lee H, Armstrong FA, Söll D. Selective cysteine-to-selenocysteine changes in a [NiFe]-hydrogenase confirm a special position for catalysis and oxygen tolerance. *Proc Natl Acad Sci U S A* [Internet]. 2021 Mar 30 [cited 2023 Apr 20];118(13):e2100921118. https://doi.org/10.1073/PNAS.2100921118/SUPPL_FILE/PNAS.2100921118.SAPPDF PMID: 33753519.

Publisher's Note

Springer Nature remains neutral with regard to jurisdictional claims in published maps and institutional affiliations.